Atmos. Meas. Tech. Discuss., doi:10.5194/amt-2016-85, 2016
Manuscript under review for journal Atmos. Meas. Tech.
Published: 12 May 2016

Atmospheric Measurement Techniques Discussions

Ceilometer evaluation of the East Mediterranean summer boundary layer height – First study of two Israeli sites

L. Uzan[12], S. Egert[1], P. Alpert[1]

[1]Department of Geosciences, Raymond and Beverly Sackler Faculty of Exact Sciences, Tel-Aviv University, Tel Aviv, 6997801, Israel.
[2]Associations of Towns for Environmental Protection (Sharon-Carmel), Hadera, 3850100, Israel
Correspondence to: L. Uzan (Leenesu@gmail.com)

Atmos. Meas. Tech. Discuss., doi:10.5194/amt-2016-85, 2016
Manuscript under review for journal Atmos. Meas. Tech.
Published: 12 May 2016

Atmospheric Measurement Techniques Discussions

Abstract. Active remote sensing instruments such as ceilometers have been shown to be potentially useful for the investigation of the behavior of the atmospheric mixing layer height (MLH). For the first time, high resolution measurements of backscatter intensity from two CL31 ceilometers situated inland and onshore of Israel, enable to evaluate the diurnal MLH in the east Mediterranean region. Although the Israeli summer synoptic conditions are considered quite stable, results for the summer season (July-August 2014) showed the inland MLH was about 200 m higher than the onshore site only 7.5km apart. The prevailing influence of the sea breeze front (SBF) as it progresses inland is presented by the ceilometer plots. A good comparison is found between the radiosonde profiles and the adjacent ceilometer in the inland site of Beit Dagan. The ceilometers revealed significant cloud cover throughout the day with higher presence onshore, in contrary to the often assumed clear skies of the Israeli summer. For further research, a prospective on cloud thickness, inland and onshore, will serve to define the inversion intensity as the MLH evolves.

Keywords: Aerosols, Mixed layer height, Ceilometer

1. Introduction

A sound understanding of atmospheric boundary layer (ABL) main properties, such as height and temporal evolution, and the factors affecting these properties, is essential for meteorological forecasting, climate studies and particularly air quality assessments (Angelini et al., 2009). A characterization of mixing layer height (MLH) diurnal evolution is most crucial in regulating the extent of air pollution dispersion (Tang, 2015; Uzan and Alpert, 2012; Ludwing, 1983). In order to develop suitable criteria to warn from adverse ambient conditions, it is important to evaluate the processes governing the ambient atmospheric variations. Usually, such predictions are done by numerical weather prediction models (Leventidou et al., 2013). However, the feasibility and accuracy of these models is attributed to calibration by comparison to actual field measurements (Kamp et al., 2010; Lieman and Alpert, 1993). Most beneficial are direct measurements in high temporal and spatial resolution. Such measurements enable to emulate atmospheric phenomena and distinguish evolvement at its early stage. Previous studies suggest using more than one remote sensing technique to overcome the deficiencies of individual instruments (Cohn and Agenvine, 2004; Emeis et al. 2008). In such research, it must be taken into account the different physical technologies of each instrument since instruments respond differently to meteorological conditions. Each instrument has advantages and limitations in measuring various meteorological parameters. Overall, a combination of several techniques offers the opportunity to follow the whole diurnal cycle of MLH (Dayan and Lifshitz-Golden, 2002). Meteorological measurements of the temperature profiles in Israel are performed by radiosondes (RS) twice a day at 00 coordinated universal time (UTC) and 12 UTC in a single point (Beit Dagan, flat terrain, 7.5km from shoreline). Profiles from a single radiosonde provide only rough estimates of the MLH due to the arbitrary ascents in thermals or between thermals (Dayan and Koch, 1992; Leventidou et al., 2013). Stationary ground based remote sensing are more frequent but detect the MLH

Atmos. Meas. Tech. Discuss., doi:10.5194/amt-2016-85, 2016
Manuscript under review for journal Atmos. Meas. Tech.
Published: 12 May 2016

Atmospheric Measurement Techniques Discussions

temporal resolution rather than spatial horizontal properties. This research focuses on two CL31 ceilometers, one onshore and the other inland, first to be deployed among an array that is gradually being established in Israel. It was interesting to find difference in the average diurnal MLH between the two measuring sites only 7.5 km apart (Fig. 1). This paper will show first results for the summer of 2014 based on the main summer months (July – August). Instrument description is given in section 2, the area of research is described in section 3, sections 4, 5 and 6 present the methodology, results and conclusions, accordingly.

2. Instrument description – CL31 Ceilometer

Research from the last decade (Schween et al., 2014; Haeffelin et al., 2012; Emeis et al., 2008; Emeis and Schäfer, 2006; Münkel et al., 2004; Cohn and Agenvine, 2000) analyzed the vertical aerosol distribution as it adapts rapidly to the changing thermal structure of the boundary layer. This characteristic allows aerosols to be used as tracers for the determination of the atmospheric MLH. Active remote sensing instruments, such as ceilometers, produce backscatter intensity plots relative to the atmospheric aerosol content and therefore potentially are useful for investigation of the behavior of the atmospheric MLH. The Vaisala CL31 ceilometer is a pulsed elastic micro lidar employing an Indium Gallium Arsenide (InGaAs) laser diode transmitter technology of near infrared wavelength (910nm ±10nm at 25˚C). In order to provide sufficient signal to noise ratio (SNR), tens of thousands of short pulses are emitted to the atmosphere in a measuring interval of 2s. The backscatter intensities collected by an avalanche photo diode (APD) receiver are averaged to produce an individual backscatter profile (raw data) within a reporting interval (2-120s). In this study, the onshore ceilometer produces backscatter intensity resolution every 16s and 10m between 0-4.5 km and the inland every 15s and 10m between 0-7.7km. The summer MLH in Israel is mainly under 1000m AGL (Uzan and Alpert, 2012; Dayan and Lifshitz-Golden, 2002; Lieman and Alpert, 1993) therefore CL31 ceilometer with a 15 -16s reporting time interval is sufficient (Kotthaus et al., 2016; Wiegner et al., 2014).

3. Research Area

Israel is located in the east Mediterranean (EM) between 29-33°N north to the desert belt (Fig. 1). The hot summer season is humid in the coastline (west) and dries inland (east and south) with a prevailing synoptic system of Persian trough (Alpert et al., 2004). Here we focused on the summer MLH from two measurement sites; onshore in Tel Aviv (TLV) and inland in Beit Dagan (BD). The onshore TLV ceilometer is located 5m AGL and 50m from shoreline of the central coast of Israel. The inland BD ceilometer is located 33m AGL and 7.5km from shoreline, 12 km southeast to TLV ceilometer. Details of the measuring sited are given in Table 1. The area of both locations is considered as flat terrain and humid up to 80% relative humidity (RH). Figure 2 shows a wider range in RH values in the inland BD site due to the transition between day and night as a function of distance from the coast. The Sea salt aerosols, defined as hygroscopic atmospheric particles, grow as function of water vapor content and influence the extinction coefficient of the ceilometer signal (Fukushima et al., 2016; Wiegner et al., 2015). With regard to the wavelength of the backscatter signal, Wiegner (2014) determines the extinction

Atmos. Meas. Tech. Discuss., doi:10.5194/amt-2016-85, 2016
Manuscript under review for journal Atmos. Meas. Tech.
Published: 12 May 2016

Atmospheric Measurement Techniques Discussions

coefficient of CL31 ceilometer signal (910nm) should be corrected for water vapor. The data presented here is based on the first CL31 ceilometers operating in Israel which have not yet referred to backscatter extinction corrections and routine calibration, therefore should be taken into account. However, Weigner (2014) points out that aerosol layer presence and extension, utilized for MLH detection, can be determined from uncalibrated ceilometer data.

4. Methodology

The daily ceilometer output profiles, produced as ".his" files, were processed as daily plots for a first impression in order to define the height range of the MLH evaluation. An example of the process for the 21.08.2014 is given in Figure 3. The ceilometer TLV backscatter intensity plot between 0-4.5km reveals the MLH is less than 2km AGL (Fig.3a). Therefore, the next stage focuses on the height range of 0-2km. To reduce the noise effect visible in raw data plots, the backscatter intensity profiles were averaged by 15min running average for the relevant height range (Fig. 3b). The profiles were hourly (or half hourly) averaged (Fig. 3c) and normalized for wavelet covariance transforms (WCT) calculations. WCT is a measure of the similarity of the range-corrected lidar backscatter signal and the Haar function. The Haar function calculates irregularities along a profile by defined steps (Baars et al., 2008) as given in Eq. (1):

$$h\left(\frac{z-b}{a}\right) = \begin{cases} +1, & b-\frac{a}{2} \le z \le b, \\ -1, & b \le z \le b+\frac{a}{2} \\ 0, & elsewhere \end{cases} \quad (1)$$

Where z is the measurement height, a is the extent of the step function chosen by the user, b is the location of the step along the height profile.

Following Eq. (1) the WCT calculation is given in Eq. (2):

$$W_f(a,b) = \frac{1}{a}\int_{Zb}^{Zi} f(z)h\left(\frac{z-b}{a}\right)dz \quad (2)$$

Where z is the measurement height, a is the symmetrical boundaries of step function where the length of each step is determined by $a=n*\Delta z$, Δz is the height resolution of the lidar signals, b is the location of the step along the height profile, *Zb and Zi* - are the lower and upper limits of the lidar return signal profile respectively and *f(z)* is the range-corrected lidar backscatter signal

In our research, the length of each step (a) is determined by the backscatter intensity depending on the ceilometer type, its settings and the meteorological conditions. Each hourly (or half hourly) profile was normalized by the highest backscatter intensity value received within the mixed layer. The WCT was implanted in a MATLAB script to calculate peak values along

Atmos. Meas. Tech. Discuss., doi:10.5194/amt-2016-85, 2016
Manuscript under review for journal Atmos. Meas. Tech.
Published: 12 May 2016

Atmospheric Measurement Techniques Discussions

the normalized profiles by three scenarios simultaneously: multi cloud layers, single cloud layer and clear skies. The evaluation output was summed and expressed as the diurnal MLH (black line laid upon the 15 min running average plot in Fig. 3d). Finally the calculated MLH was compared between ceilometers and radiosonde profiles (dealt in Sect. 5). To analyze the diurnal variations in the MLH, each day was referred by the prevailing synoptic system, geostrophic wind, SBF entrance time and cloud presence.

In order to produce, validate and improve the aforementioned WCT algorithm, each diurnal MLH was compared to Hysplit back trajectories (500m, 1,500m, 3,000m AGL ending at 23:00), National Centers for Environmental Predictions (NCEP) synoptic maps (1000mb, 850mb, 700mb maps at 00Z, 06Z, 12Z, 18Z), Tel Aviv University (TAU) Desert Dust Model and the Weather Research and Forecasting model (WRF version 3.5.1). The comparison emphasized the low resolution of the latter data set, compared to the high resolution ceilometer output.

For example, figure 4 presents the dust storm evolution over Israel on the 02.03.14 measured by ceilometers. The dust concentrations calculated by the WRF model (10km resolution) produced results for particulate matter with aerodynamic diameter under 10μm (PM10). The WRF model revealed a dust front over 1,000m AGL around 09:00 local standard time (LST). At March (spring season) the LST equals UTC+2. The onshore (TLV) and inland (BD) ceilometers revealed dust penetrating downward at 05:00 LST creating a dust front up to 500m AGL. Furthermore, a dust "tail" visible in the ceilometer plots at 800 m ABL before 05:00 LST had not been identified by the WRF model. The WRF model calculated a dust "torch" between 1,200-2,500m AGL at 10:00-13:00 LST. This phenomenon was visible mainly in the inland BD ceilometer 3 hours earlier, between 07:00-09:00 LST at lower heights of 600-1,500m AGL. We believe these major differences, which are most important for aviation, are also due to the WRF run limitations of resolution (10km) and dust source input (only natural dust).

Good correlation was found between the first 10m AGL backscatter intensity of TLV ceilometer and the adjacent ground station PM10 monitoring. The positioning and distance between the ceilometer and the PM10 monitoring sited is illustrated in figure 5. Examples are given in figures 6 and 7 for the dates 01.08.14 and 12.08.14. However, we must note we have detected constant noise at 30m AGL in the BD ceilometer and 50m AGL in the TLV ceilometer. One explanation is due to the ceilometer positioning and settings.

5. Results

A summary of the diurnal average summer MLH as detected by the onshore and inland ceilometers is presented in figure 8. The high resolution (hourly averaged) MLH demonstrates the following process: After sunrise (around 03:00 UTC) the ground warms up and the surface nocturnal boundary layer breaks. Thermals inflate the ABL (around 05:00 UTC) recreating the morning mixed-layer. A developed SBF moves inland, reducing the thermal buoyancy consequently causing subsidence of the MLH. Figure 8 demonstrates the prevailing influence of the SBF as it enters an hour earlier in the shoreline (TLV) compared to inland (BD). Lieman and Alpert (1993) calculated similar results based on a 3D mesoscale mathematical model. Uzan and Alpert (2012) showed the same results for the summer season from the central coast of Israel by a Lap-3000 acoustic radar

Atmos. Meas. Tech. Discuss., doi:10.5194/amt-2016-85, 2016
Manuscript under review for journal Atmos. Meas. Tech.
Published: 12 May 2016

Atmospheric Measurement Techniques Discussions

continues measurements of wind speed, wind direction and virtual temperature profiles. In contrary to former research of Dayan and Lifshitz-Golden (2002) indicating the inland BD MLH is 50m higher than an onshore site 3.5km from shoreline. Here, the inland BD MLH tends to be 200 m higher than the onshore TLV MLH due to the less developed and therefore weaker thermals only 50m from shoreline compared to the 7.5km inland site. Another point is the stronger temperature gradient onshore compared to inland (Atkinson, 1981). After sunset, around 16:30 UTC, the SBF and thermals weaken, the MLH subsides by the summer high pressure synoptic system prevailing in the free atmosphere (Alpert et al., 2004). As a consequence, the onshore and inland MLH coincide to the average height of 650m AGL until sunrise.

Examples of a single day evolvement are given in Figures 9 and 10. For each day, the TLV SBF entrance time was analyzed by Alpert and Rabinovich-Hadar (2003) method based on the ambient temperature, relative humidity, wind speed and wind direction from a ground monitoring station situated 2km from Tel Aviv shoreline. In order to avoid deviation in the daily heat balance, only days with no clouds were analyzed. Unfortunately, it appeared clear days on both sites, onshore and inland, were scarce due to an uncharacteristic cloudy summer of 2014. The SBF progress inland was assessed by the wind speed at 300m AGL as suggested by Atkinson (1981). The wind speed of 5m/s was estimated by the radiosonde profiles of 12 UTC in the BD site and the Lap-3000 acoustic radar profiles situated 3.5km from shoreline in the central coast of Israel (Uzan, 2007). With a 5m/s wind speed it would take the SBF approximately 25min to advance from the TLV onshore site, 7.5km inland to the BD site. This calculation fits accurately with the time the MLH begins to subside on 20.08.2014 (Fig. 9). The SBF enters the TLV site at 6:00 UTC causing subsidence at 06:30 UTC in the BD MLH. On the other hand, 13.08.2014 reveals a different development (Fig. 10). The SBF enters the TLV site at 6:00 UTC and is identified in the BD site at 08:00 UTC, an hour and a half later than calculated. One explanation is referred to the intensity and direction of the gradient wind which can hinder SBF development. The 925mb NCEP synoptic maps at the SBF approximated entrance time (06:00 UTC) reveal this affect with northern wind of 4.3m/s compared to the weak north-west wind of 1.6m/s on the 20.08.2014 (Table. 2). Moreover, the TLV MLH on the 13.08.2014 began at 400m AGL while on the 20.08.2014 an inflated MLH of about 650m AGL prevailed. The stable atmosphere of 13.08.14 results with a lower MLH and suppresses the sea breeze vertical circulation, reducing the SBF intensity and progress. The influence of the atmospheric stability and the gradient wind on the formation of the SBF is well explained by Atkinson (1981).

To verify our MLH calculations, we compared the daily ceilometer data shown in Fig. 8 with the RS profiles (Fig. 11 and 12). The RS is launched twice a day (00 and 12 UTC) by the Israeli Meteorological Service (IMS), luckily located right next to the BD ceilometer. Definition of the MLH from the RS profiles was based on Stull 1988, and referred to temperature (inversion layer), relative humidity (significant drop), wind speed (strong wind shear), and virtual temperature (increase aloft). Inevitably, the correlation of MLH between in the BD site was higher with R^2=0.82 for 12 UTC and R^2=0.79 for 00 UTC, than between the TLV site with R^2=0.62 for 12 UTC and R^2=0.63 for 00 UTC (Fig. 13 and 14). Some of the variations between the RS and the ceilometers, were due to large gaps of hundreds of meters in the RS profiles, and therefore an approximately estimation of the inversion height was not possible. Overall, the comparison of RS profiles inland and onshore comply with figure 8 showing that the TLV MLH tends to be lowest during daytime and the MLH from both sited collide during the night.

Atmos. Meas. Tech. Discuss., doi:10.5194/amt-2016-85, 2016
Manuscript under review for journal Atmos. Meas. Tech.
Published: 12 May 2016

Atmospheric Measurement Techniques Discussions

Another issue is significant difference in cloud coverage between the two measuring sited (example in Fig. 15). Cloud coverage plays an important role in the heat balance therefore influence the MLH development. In Israel cloud detection is done mainly by observation which is limited in space (numerous observation points) and time (impossible at night hours). In order to overcome the luck of cloud cover data in our region, we have analysed the daily ceilometer plots between July-August 2014 by four time periods: before sunrise (01:00-03:00 UTC), after sunrise (04:00-09:00 UTC), daytime (10:00-16:00 UTC) and after sunset (17:00-23:00 UTC). Each time period was scored for cloud coverage as follows: 1-for consecutive cloud cover, 0.5-for sporadic cloud cover and 0-for no clouds. Results (illustrated in figure 16) reveal that after sunset the percent of clouds was higher on July compared to August, significantly in the inland site (BD). This can explain the lower MLH of BD site on July compared to August due to weaker thermals. Overall, the onshore site (TLV) was found to be cloudier than the inland site (BD).

6. Conclusions

Ceilometers are beneficial in monitoring the atmosphere by providing high resolution measurements. The ceilometers output is influenced by cloud presence and all types of atmospheric particulate matter, including natural dust and anthropogenic aerosols. For the first time, a comparison done by simultaneous measurements from ceilometers onshore and inland in flat terrain showed differences of 200m between the onshore and inland MLH (7.5km apart) mainly during the day hours. Verification by in situ adjacent RS measurements complies with the MLH ceilometer detection. The ceilometer measurements revealed a significantly cloudy summer of 2014, contrary to the characteristic clear sky commonly defined. Further investigation of the cloud types and layers will aid to interpret the thermal heat flux difference influencing the MLH evolvement. The number of operative ceilometers in Israel is growing rapidly offering detailed information of the local evolution pattern of the MLH height in several points. Ceilometer MLH assessment can be utilized to assist in estimation of pollution risk analysis and serve as test profiles for dust models.

Acknowledgements

We wish to thank the Israeli Meteorological Service (IMS) and the Israeli Air force (IDF) for the data and collaboration. Special thanks to Nir Stav (IMS) for his fruitful advice, Anat Baharad (Tel Aviv University) for the assistance with the MATLAB scripts and Pavel Kunin (Tel Aviv University) for the WRF model runs.

Atmos. Meas. Tech. Discuss., doi:10.5194/amt-2016-85, 2016
Manuscript under review for journal Atmos. Meas. Tech.
Published: 12 May 2016

Atmospheric Measurement Techniques Discussions

References

Alpert P., Osetinsky I., Ziv B. and Shafir H.: A new seasons definition based on the classified daily synoptic systems: An example for the Eastern Mediterranean, Int. J. Climatol. 24, 1013-1021, 2004.

Alpert P., and Rabinovich-Hadar M.: Pre- and post- frontal lines - A meso gamma scale analysis over south Israel, J. Atmos. Sci., 60, 2994-3008, 2003.

Atkinson B. W.: Meso-scale atmospheric circulation, Academic press, London, 495p, 1981.

Atmospheric sounding: http://weather.uwyo.edu/upperair/ sounding.html

Angelini F., Barnaba F., Landi C.T., Caporaso L., and Gobbi P.G.: Study of atmospheric aerosols and mixing layer by lidar. Radiat. Prot. Dosimetry, 137,275-279, doi: 10.1093/rpd/ncp219, 2009.

Baars H., Ansmann A., Engelmann R. and Althausen D.:Continuous monitoring of the boundary-layer top with lidar, Atmos. Chem. Phys., 8, 7281-7296, 2008.

Gan Chuen-Meei, Wu Y.H., Gross B.M., Arend M., Moshary F. and Ahmed S.: A comparison of estimated mixing height by multiple remote sensing instruments and its influence on air quality in urban regions, IGARSS, IEEE International Geoscience and Remote Sensing Symposium, Honolulu Hawaii USA, 25-30 July 2010, 730-733, 2010.

Cohn S.A., Angevine W.A.: Boundary layer height and entrainment zone thickness measured by lidars and wind-profiling radars, J. Appl. Meteor. 39, 1233-1247, 2000.

Dayan, U. and Koch J.: A synoptic analysis of the meteorological conditions affecting dispersion of pollutants emitted from tall stacks in the coastal plain of Israel, Atmos Environ., 26A, No.14, 2537-2543, 1992.

Dayan U., Lifshitz-Golden B., and Pick K.: Spatial and structural variation of the atmospheric boundary layer during summer in Israel-profiler and rawinsonde measurements, Amer. Meteo. Sco. 41,447-457,2002.

Emeis S., Schäfer K.: Remote sensing methods to investigate boundary-layer structures relevant to air pollution in cities, Bound. Lay. Meteor. 121,377-385,doi:10.1007/s10546-006-9068-2, 2006.

Emeis S., Schäfer K. and Münkel C.: Surface-based remote sensing of the mixing-layer height – a review, Meteor. Zeits. 17 , 621-630, doi: 10.1127/0941-2948/2008/0312 2008.

Fukushima S., Zhang D., Shibata T., Katagiri S. and Hayasaka T.:Dependence of backscattering coefficients of atmospheric particles on their concentration and constitution under dry and humid conditions at southwestern Japanese coast in spring, Aerosol Air Qual. Res.16, 1294-1301,2016.

Haeffelin M., Angelini F., Morille Y., Martucci G., Frey S., Gobbi G. P., Lolli S., O'Dowd C. D., Sauvage L., Xueref- Rémy I., Wastine B., and Feist D. G.: Evaluation of mixing height retrievals from automatic profiling lidars and ceilometers in view of future integrated network in Europe, Bound. Lay. Meteor. 143 ,49-75, 2012.

Kotthaus S., O'Connor E., Münkel C.,Charlton-Perez C., Gabey M. A. and Grimmond B. S.: Recommendations for processing atmospheric attenuated backscatter profiles from Vaisala CL31 ceilometers, Atmos. Meas. Tech. Discuss.in review, doi:10.5194/amt-2016-87,2016.

Leventidou E., Zanis P., Balis D., Giannakaki E., Pytharoulis I. and Amiridis V.: Factors affecting the comparisons of planetary boundary height retrievals from CALIPSO, ECMWF and radiosondes over Thessaloniki Greece., Atmos. Environ. 74, 360-366, 2013.

Lieman R.,and Alpert P.:Investigation of the planetary boundary layer height variations over complex terrain. Bound. Lay. Meteor., 62 , 129-142, 1993.

Ludwing F. L.: A review of coastal zone meteorological processes important to the modeling of air pollution, Air pollution modeling and its application IV, 7 , 225-258,1983.

Münkel C., Emeis S., Muller J. W., Schäfer K.: Aerosol concentration measurements with a lidar ceilometer: results of a one year measuring campaign, Remote sensing of Clouds and the Atmosphere VIII, 5235, 486-496, doi: 10.1117/12.511104,2004.

Schween J. H., Hirsikko A., Löhnert U., Crewell S.: Mixing layer height retrieval with ceilometer and Doppler lidar: from case studies to long-term assessment, 2014, Atmos. Chem. Physics. Discuss. 7, 4275-4319, doi:10.5194/amtd-7-4275-2014.

Stull R. B.: An introduction to boundary layer meteorology, Kluwer Academic publishers, Netherlands, 666p, 1988.

Tang G., Zhu X., Hu B., Xin J., Wang L., Münkel C., Mao G. and Wang Y.: Vertical variations of aerosols and the effects responded to the emission control: application of lidar ceilometer in Beijing during APEC, 2014, Atmos. Chem. Physics. Discuss. 15, 13173-13209, doi:10.5194/acpd-15-13173-2015,2015.

Van der Kamp D., Mckendry I.G.: Diurnal and seasonal trends in convective mixed layer heights estimated from two years of continuous ceilometers observations in Vancouver BC. Bound. Lay. Meteor, 137, 459-475, 2010.

Uzan L., Alpert P.: The coastal boundary layer and air pollution- A high temporal resolution analysis in the East Mediterranean Coast , TOASJ, 6 ,9-18,2012.

Uzan L.: Investigation of the Thermal Boundary Layer over Hadera from a LAP-3000 profiler under different synoptic and air pollution conditions, M.S. Thesis, Tel Aviv University, Israel, 93pp., 2007.

Wiegner, M. and Gasteiger, J.: Correction of water vapor absorption for aerosol remote sensing with ceilometers, Atmos. Meas. Tech., 8(9), 3971–3984, doi:10.5194/amt-8-3971-2015, 2015

Wiegner, M., Madonna, F., Binietoglou, I., Forkel, R., Gasteiger, J., Geiß, A., Pappalardo, G., Schäfer, K. and Thomas, W.: What is the benefit of ceilometers for aerosol remote sensing? An answer from EARLINET, Atmos. Meas. Tech., 7(7), 1979–1997, doi:10.5194/amt-7-1979-2014, 2014

Atmos. Meas. Tech. Discuss., doi:10.5194/amt-2016-85, 2016
Manuscript under review for journal Atmos. Meas. Tech.
Published: 12 May 2016

Atmospheric Measurement Techniques Discussions

Table 1. Ceilometer CL31 parameters

Name	Location	Time resolution	Height resolution	Height Range	Measured time
TLV "Onshore"	Tel Aviv 0.05km from shoreline 5m AGL	16s	10m	0-4.5km	UTC
BD "Inland"	Beit Dagan 7.5km from shoreline 33m AGL	15s	10m	0-7.7km	UTC+2

Atmos. Meas. Tech. Discuss., doi:10.5194/amt-2016-85, 2016
Manuscript under review for journal Atmos. Meas. Tech.
Published: 12 May 2016

Atmospheric Measurement Techniques Discussions

Table 2. Wind (U, V) in 925mb at 06:00 UTC (09:00 LST) from NCEP Reanalysis Pressure Level GrADS

Date	U-wind (m/s)	V-wind (m/s)	Dir (˚)/Speed(m/s)
13.08.2014	0.5	-4.25	007/4.3
20.08.2014	0.5	-1.5	342/1.6

Atmos. Meas. Tech. Discuss., doi:10.5194/amt-2016-85, 2016
Manuscript under review for journal Atmos. Meas. Tech.
Published: 12 May 2016

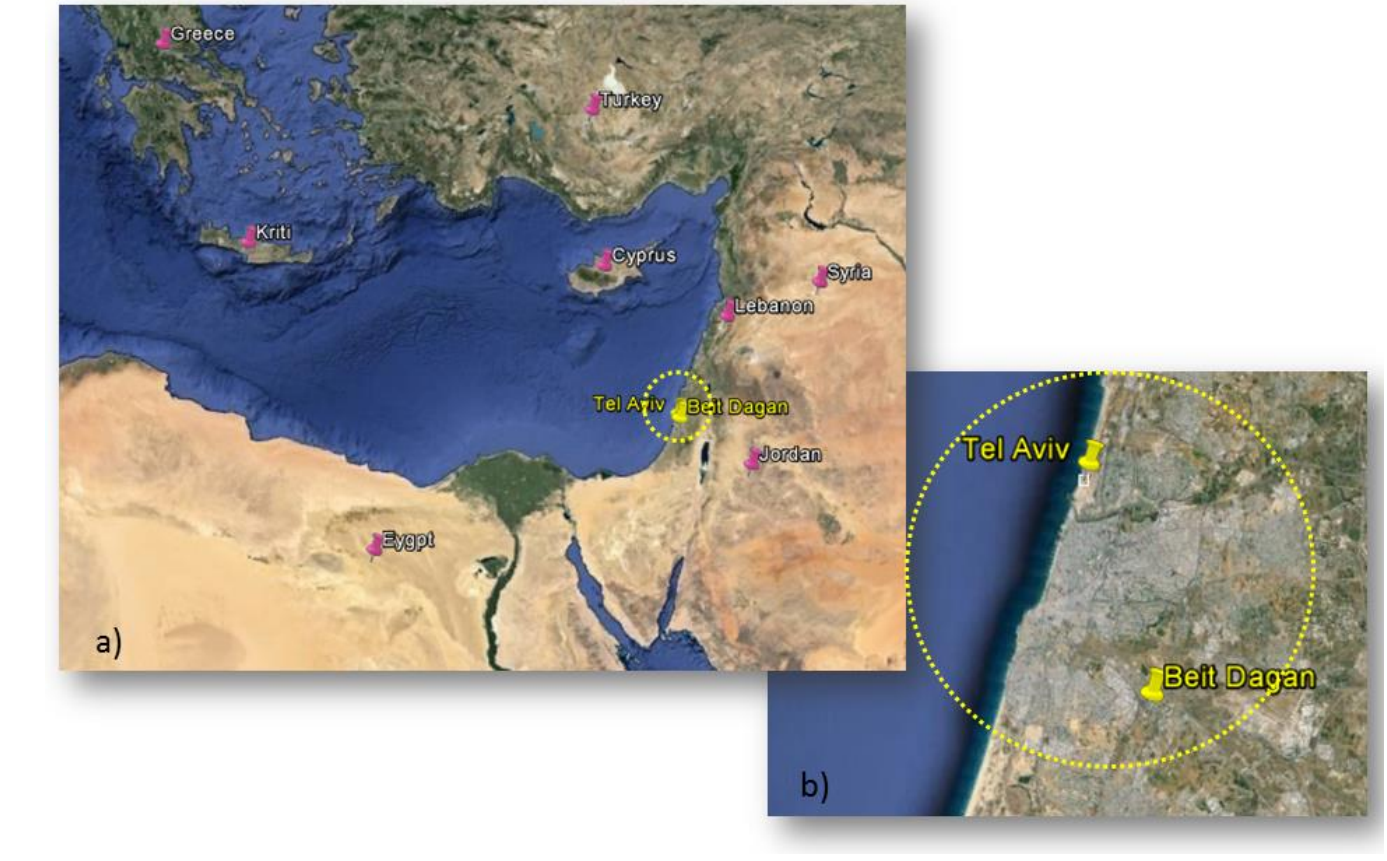

Figure 1. Google Map of east Mediterranean with indication of the ceilometers in Tel Aviv, Beit Dagan (a), Zoom-in (b).

Atmos. Meas. Tech. Discuss., doi:10.5194/amt-2016-85, 2016
Manuscript under review for journal Atmos. Meas. Tech.
Published: 12 May 2016

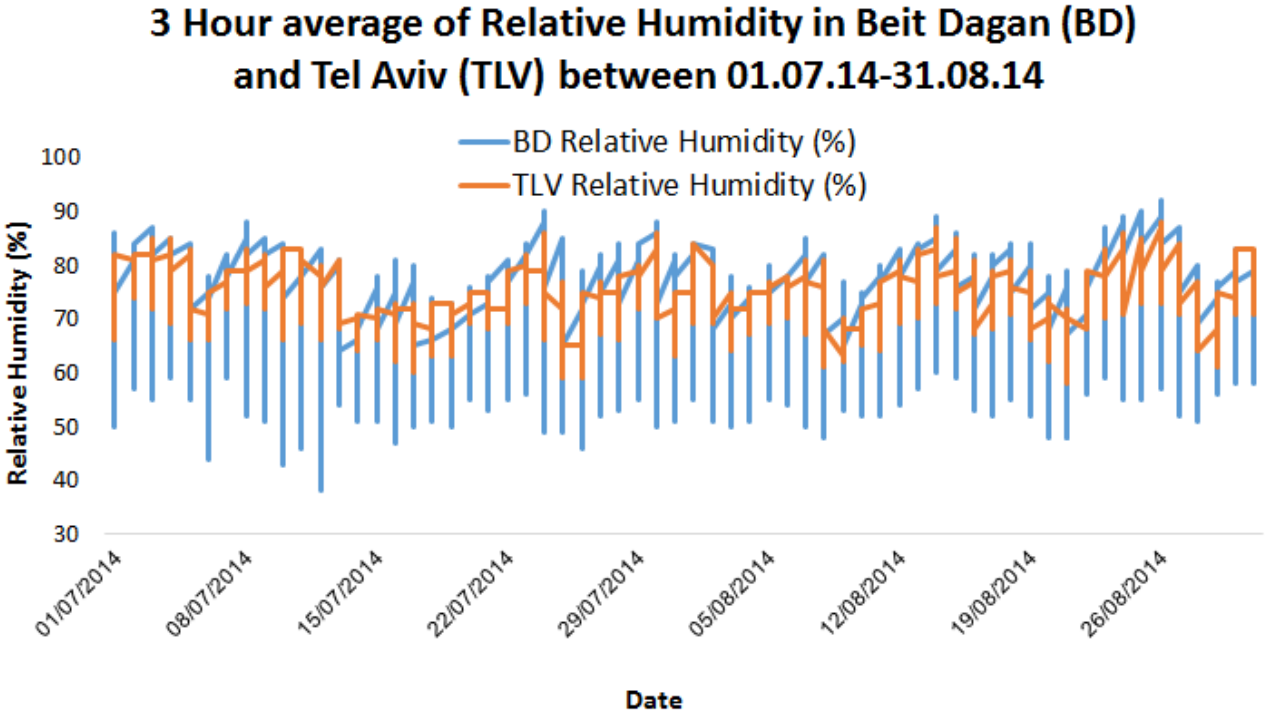

Figure 2. Relative humidity (RH) from monitoring stations near the measuring sites of the onshore ceilometer in Tel Aviv (TLV) (orange line) and the inland ceilometer in Beit Dagan (BD)(blue line). The RH monitoring stations belong to the Israeli Meteorological Service.

Atmos. Meas. Tech. Discuss., doi:10.5194/amt-2016-85, 2016
Manuscript under review for journal Atmos. Meas. Tech.
Published: 12 May 2016

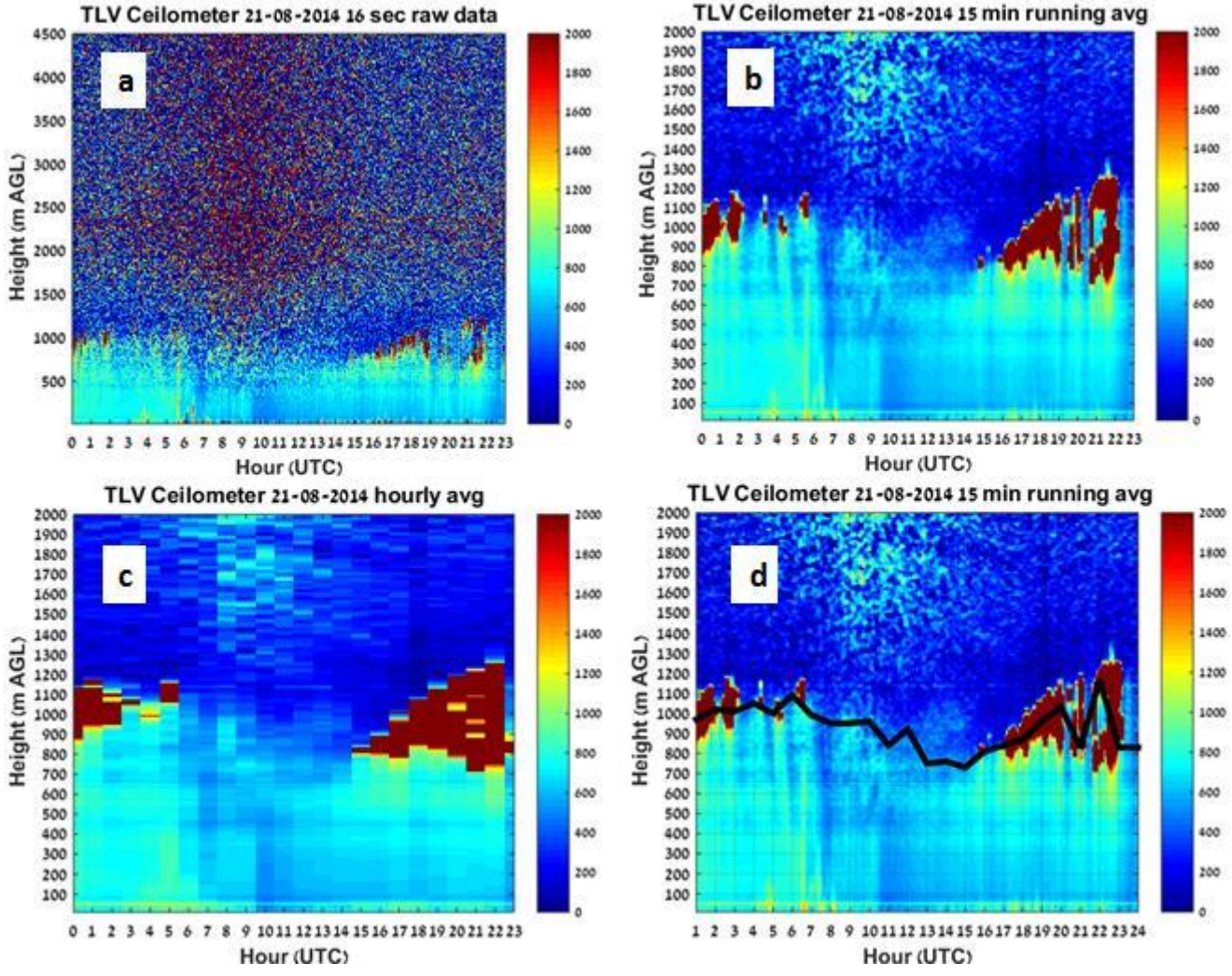

Figure 3. Stages of daily ceilometer evaluation (a) raw data plot based on backscatter intensity (units 10^{-6} m^{-1} sr^{-1}) every 16s, (b) 15min running average plot to reduce noise, (c) hourly average profiles, (d) the diurnal MLH assessed (black line) laid upon figure (b) for hours 1-24 UTC.

Atmos. Meas. Tech. Discuss., doi:10.5194/amt-2016-85, 2016
Manuscript under review for journal Atmos. Meas. Tech.
Published: 12 May 2016

Atmospheric Measurement Techniques Discussions

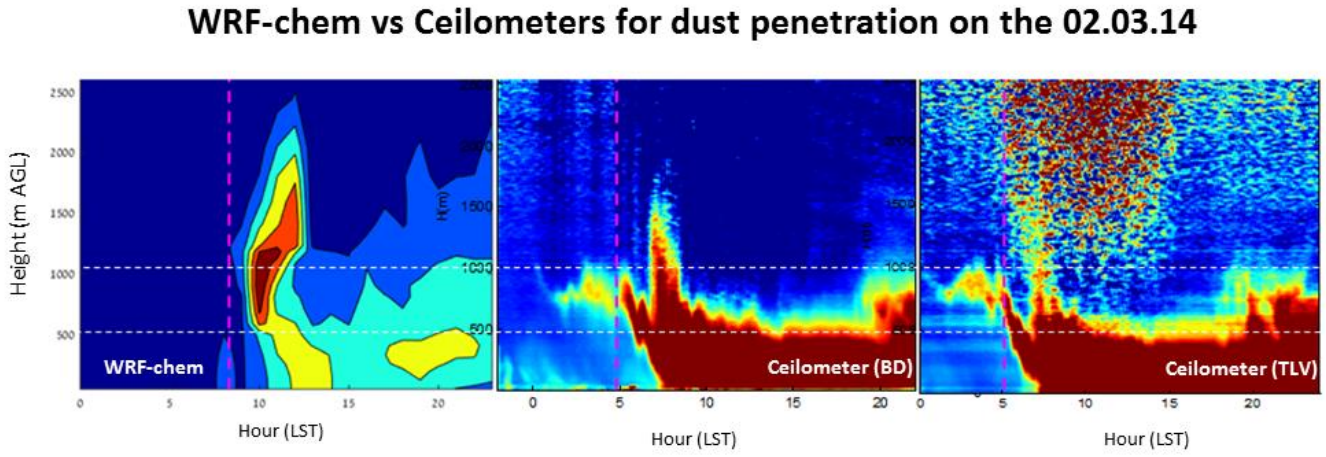

Figure 4. Comparison of the dust storm event over Israel on the 02.03.14. Dust loads of PM10 (µg/m³) processed by the WRF model version 3.5.1 for 10 km resolution (left panel), 15 min running average of inland ceilometer in Beit Dagan (middle panel) and onshore ceilometer in Tel Aviv (right panel). To facilitate the comparison between the three plots, horizontal lines were added to indicate the heights 500 and 1000 m AGL and a vertical line to indicate the entrance time of the dust front. The time scale is in local standard time (LST) which equals UTC+ 2 hrs. In the right plot, the strong backscatter intensity in the upper level between 05:00-15:00 LST is noise.

Atmos. Meas. Tech. Discuss., doi:10.5194/amt-2016-85, 2016
Manuscript under review for journal Atmos. Meas. Tech.
Published: 12 May 2016

Atmospheric Measurement Techniques Discussions

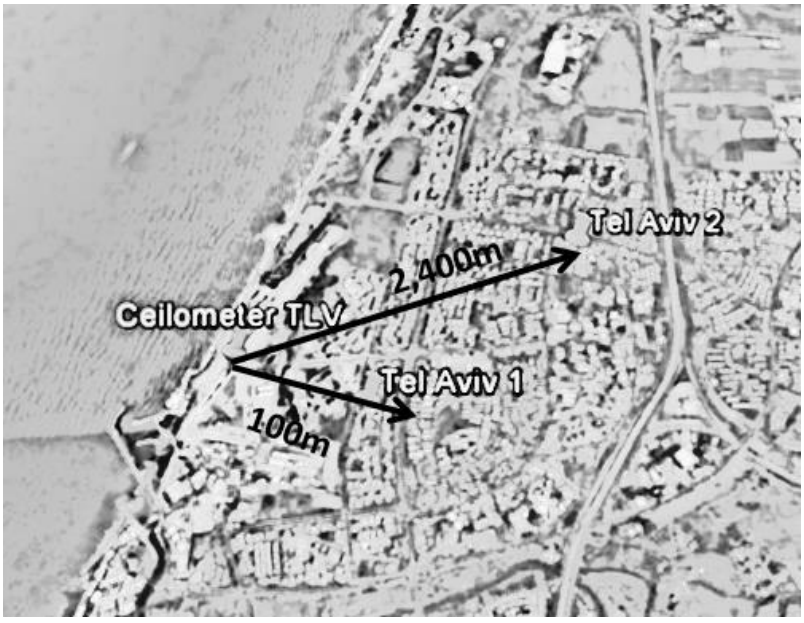

Figure 5. Google Map of southern Tel Aviv (Israel) with indication of the TLV ceilometer site, the two PM10 ground station monitoring (Tel Aviv 1, Tel Aviv 2) and their distance from the ceilometer. The monitoring stations belong to the Israeli environmental protection ministry.

Atmos. Meas. Tech. Discuss., doi:10.5194/amt-2016-85, 2016
Manuscript under review for journal Atmos. Meas. Tech.
Published: 12 May 2016

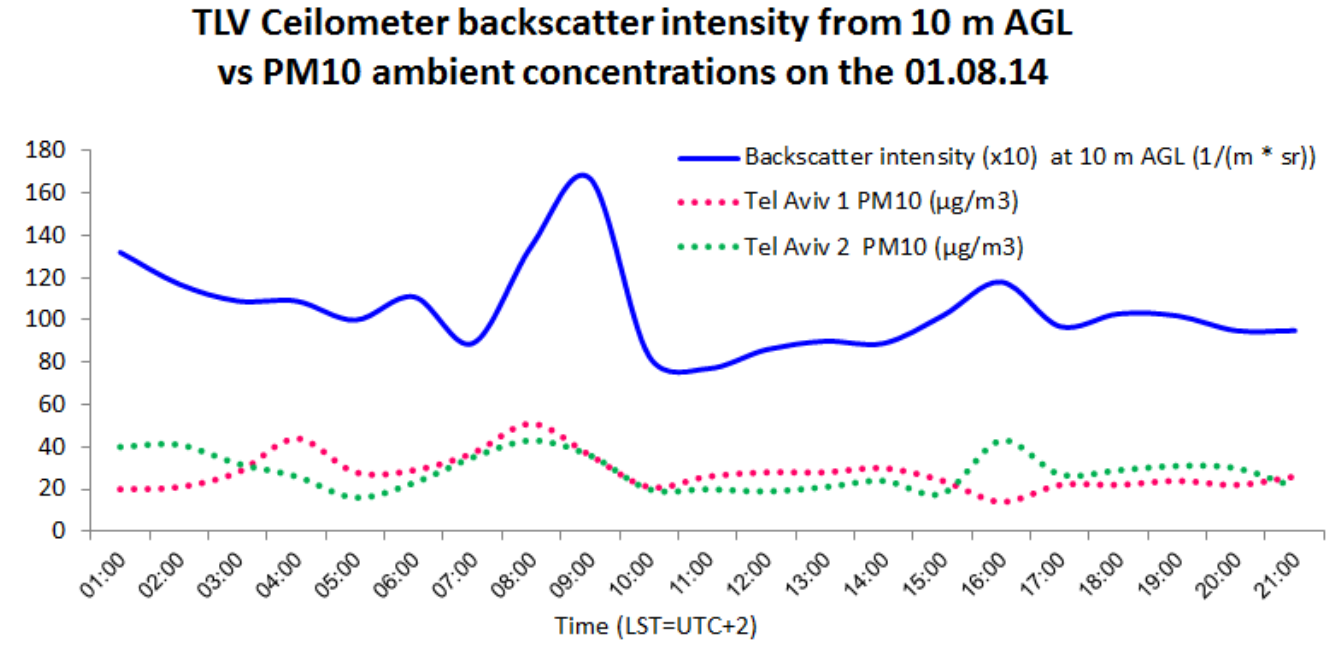

Figure 6. Hourly average on the 01.08.14 of backscatter intensity from 10m AGL measurement from the onshore ceilometer in Tel Aviv (blue line) and PM10 concentrations (dashed lines) from two ground base monitoring stations in the area (see map in figure 5).

Atmos. Meas. Tech. Discuss., doi:10.5194/amt-2016-85, 2016
Manuscript under review for journal Atmos. Meas. Tech.
Published: 12 May 2016

Atmospheric Measurement Techniques Discussions

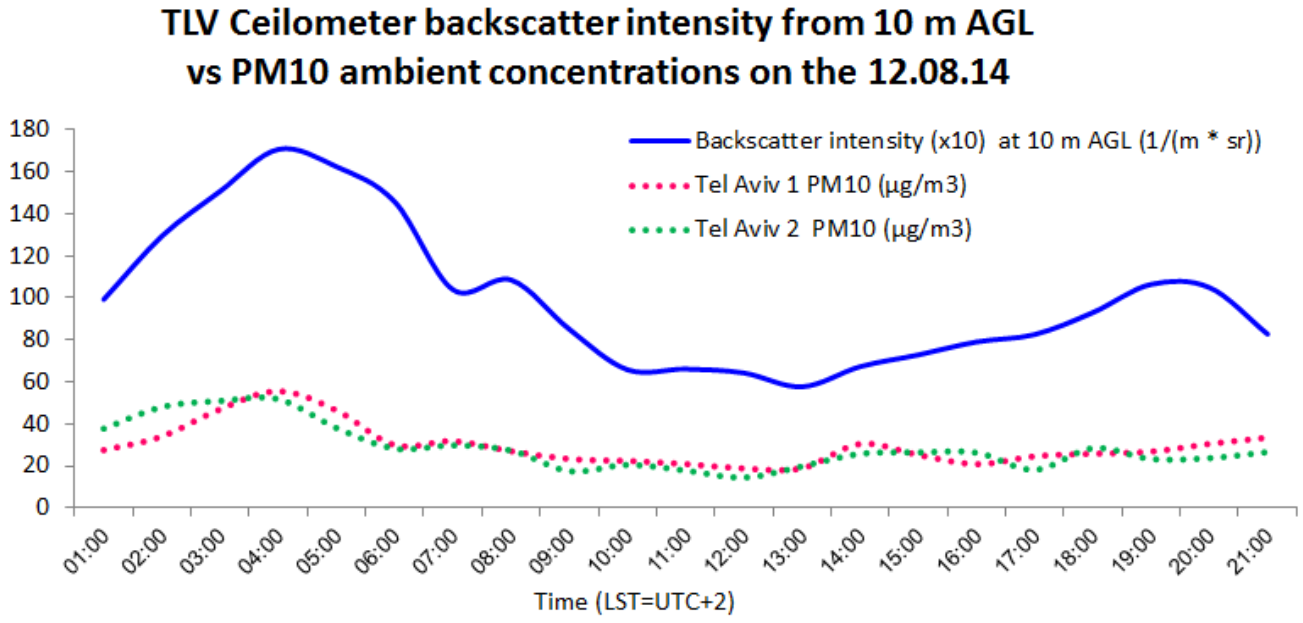

Figure 7. Same as figure 6 but for 12.08.14

Atmos. Meas. Tech. Discuss., doi:10.5194/amt-2016-85, 2016
Manuscript under review for journal Atmos. Meas. Tech.
Published: 12 May 2016

Atmospheric Measurement Techniques Discussions

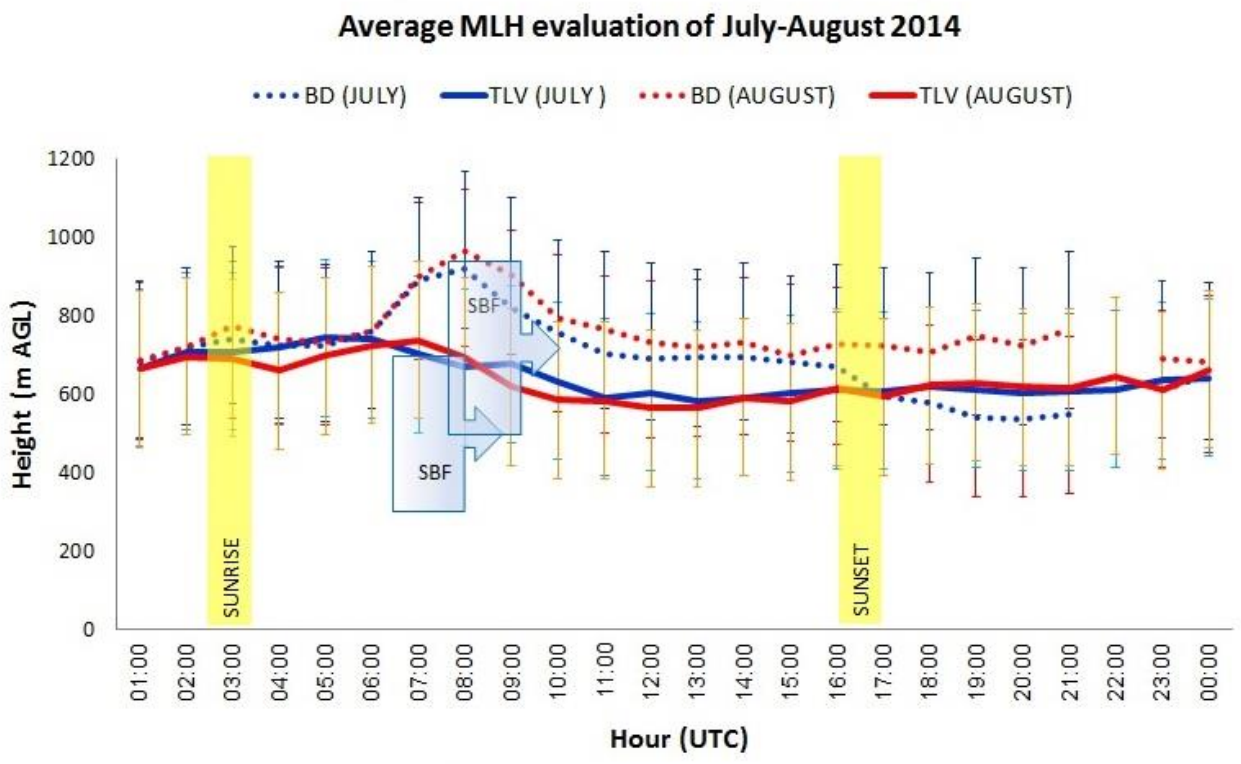

Figure 8. The hourly average MLH for the EM summer season (July – August) 2014. Blue lines are for July in BD (dashed) and TLV (solid) sites. Red lines are for August in BD (dashed) and TLV (solid) sites. TLV and BD curves are based on 19, 31 days in July and 24, 30 days in August, respectively. The plot includes error bars and time range indications of the sunrise, sunset and the SBF progress from TLV to BD.

Atmos. Meas. Tech. Discuss., doi:10.5194/amt-2016-85, 2016
Manuscript under review for journal Atmos. Meas. Tech.
Published: 12 May 2016

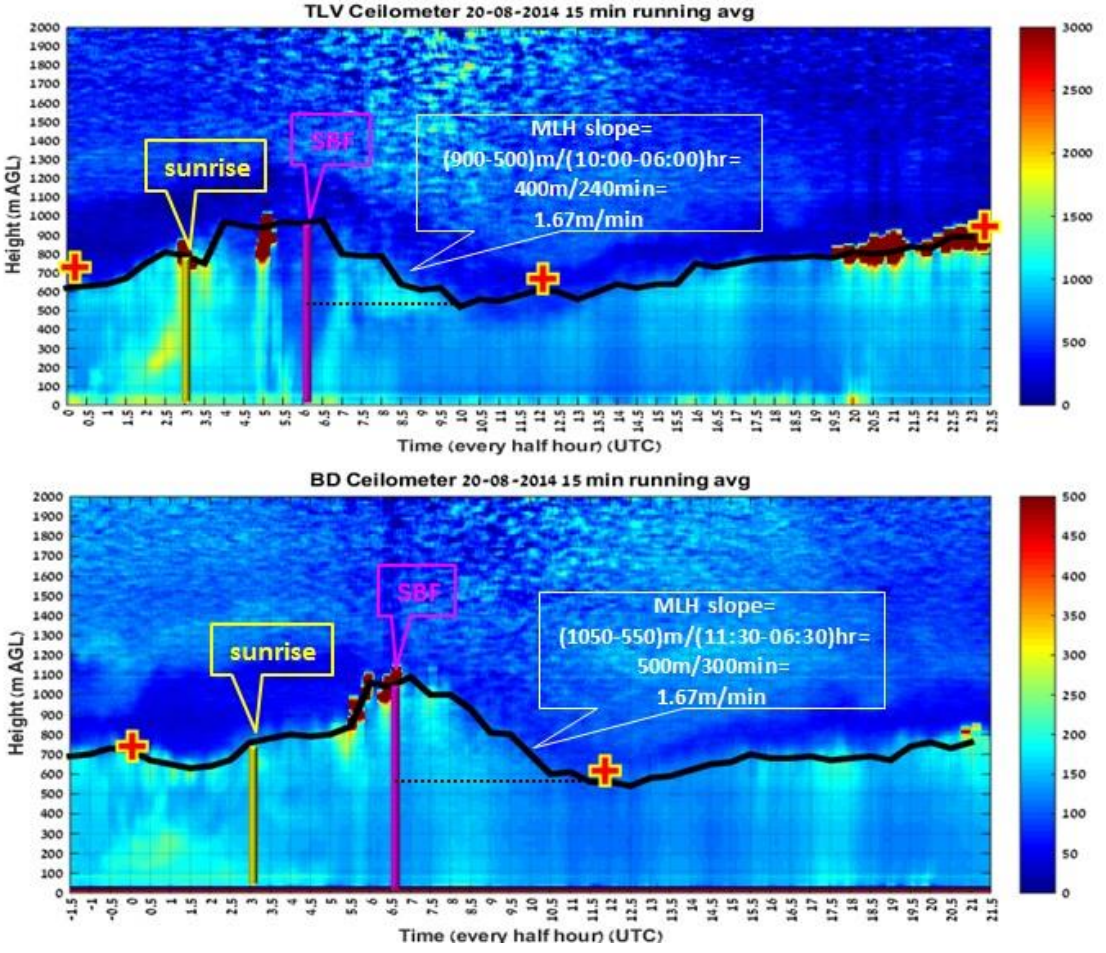

Figure 9. Diurnal MLH (solid black line) on the 20.08.2014 for BD and TLV. The MLH is implanted upon the half hourly averaged plots of backscatter intensity (units 10^{-6} m^{-1} sr^{-1}). The BD plot is shifted 2 hours to coincide with UTC time. The plot includes indications of the sunrise (yellow bar), the SBF entrance time (pink bar), MLH evaluation by radiosonde profiles at 00 and 12 UTC (red plus) and calculation of the rate of MLH subsidence due to SBF entrance.

Atmos. Meas. Tech. Discuss., doi:10.5194/amt-2016-85, 2016
Manuscript under review for journal Atmos. Meas. Tech.
Published: 12 May 2016

Atmospheric Measurement Techniques Discussions

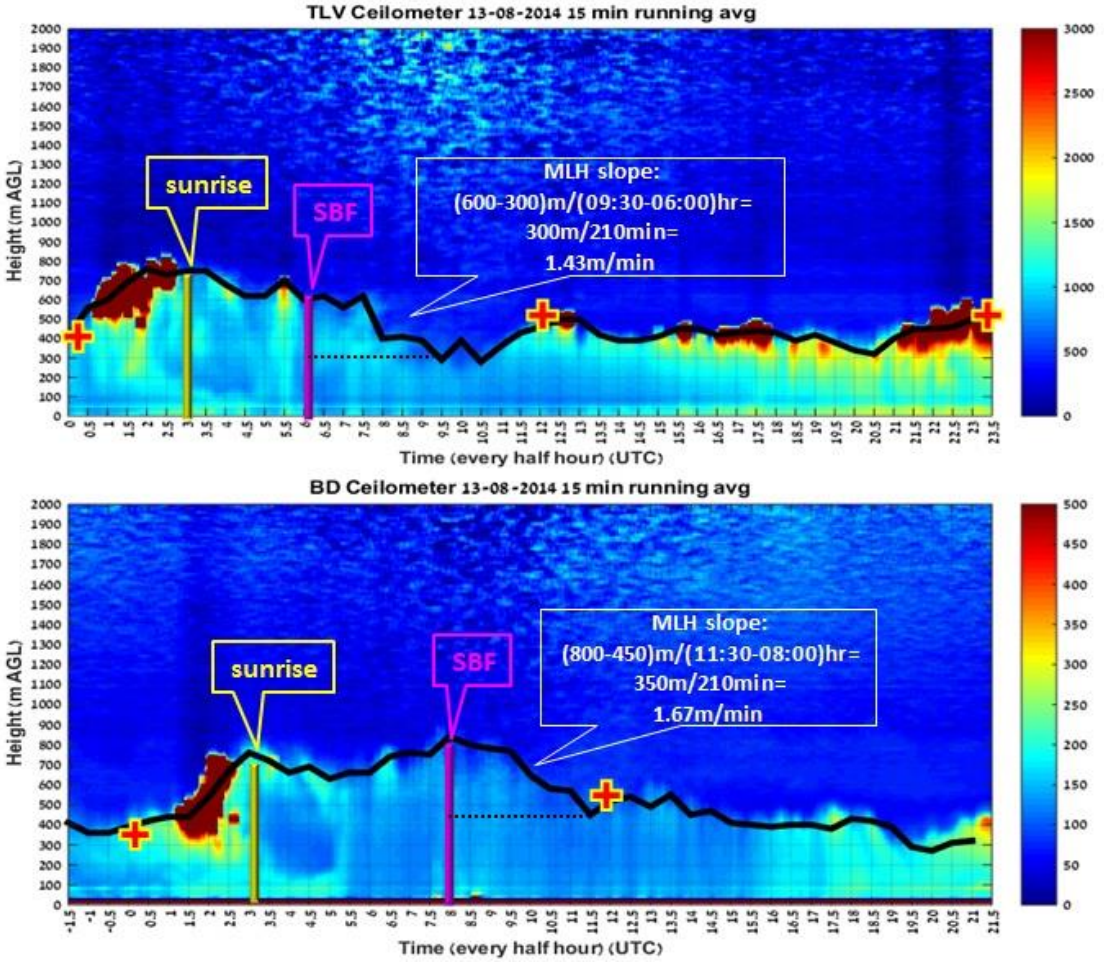

Figure 10. Same as Figure 9 but for the 13.08.2014.

Atmos. Meas. Tech. Discuss., doi:10.5194/amt-2016-85, 2016
Manuscript under review for journal Atmos. Meas. Tech.
Published: 12 May 2016

Atmospheric Measurement Techniques Discussions

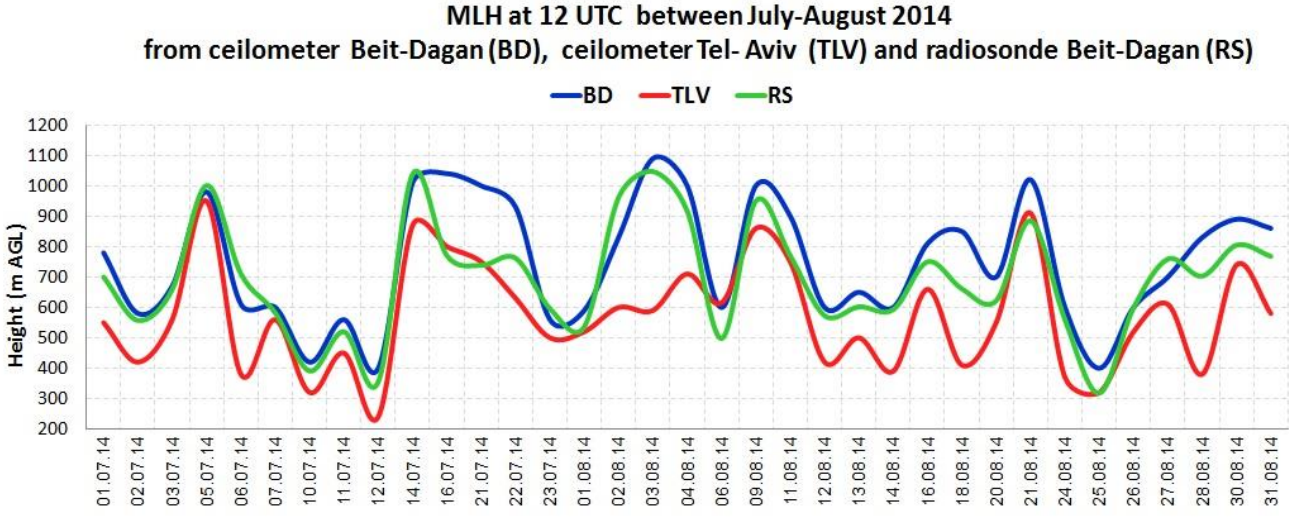

Figure 11. The diurnal MLH at 12 UTC between July – August 2014 from ceilometers TLV and BD compared to the MLH derived from the Radiosonde. The evaluation was based on 35 days between 01.07.14-31.08.14 with full data from the three instruments.

Atmos. Meas. Tech. Discuss., doi:10.5194/amt-2016-85, 2016
Manuscript under review for journal Atmos. Meas. Tech.
Published: 12 May 2016

Atmospheric Measurement Techniques Discussions

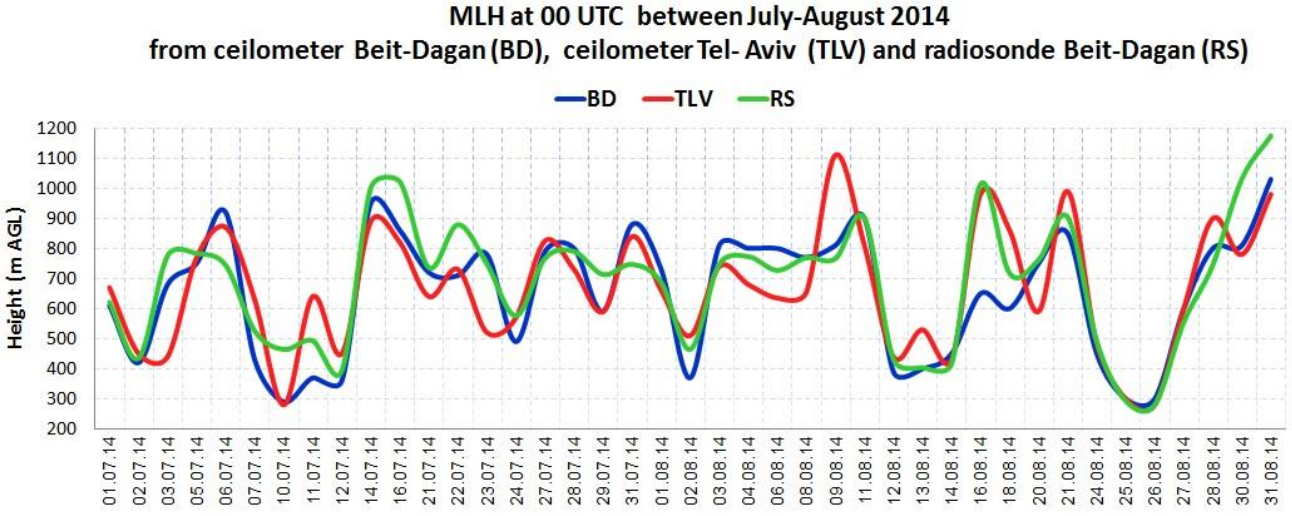

Figure 12. Same as Figure 11 but for 00 UTC based on 41 days between 01.07.14-31.08.14 with full data from the three instruments.

Atmos. Meas. Tech. Discuss., doi:10.5194/amt-2016-85, 2016
Manuscript under review for journal Atmos. Meas. Tech.
Published: 12 May 2016

Atmospheric Measurement Techniques Discussions

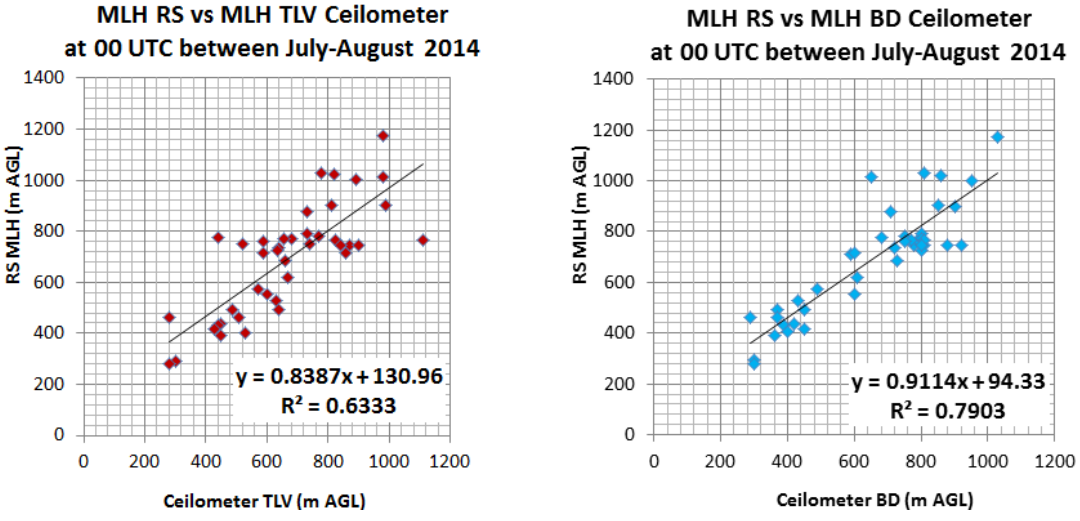

Figure 13. Correlation values between MLH estimation from radiosonde (RS) profiles at 00 UTC, the onshore Tel Aviv (TLV) ceilometer and the 7.5 km inland Beit Dagan (BD) ceilometer. The BD ceilometer is adjacent to the RS launching site.

Atmos. Meas. Tech. Discuss., doi:10.5194/amt-2016-85, 2016
Manuscript under review for journal Atmos. Meas. Tech.
Published: 12 May 2016

Atmospheric Measurement Techniques Discussions

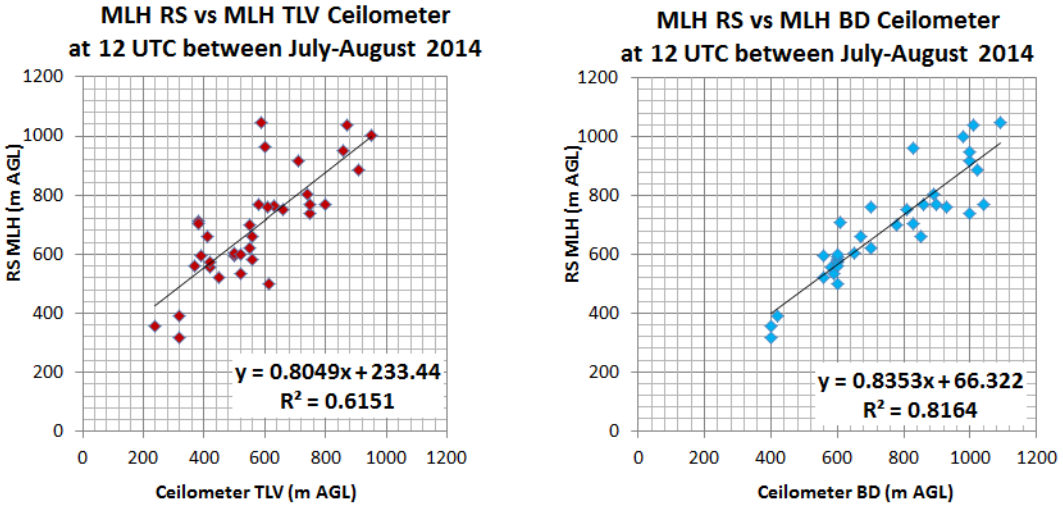

Figure 14. Same as figure 13 but for 12 UTC.

Atmos. Meas. Tech. Discuss., doi:10.5194/amt-2016-85, 2016
Manuscript under review for journal Atmos. Meas. Tech.
Published: 12 May 2016

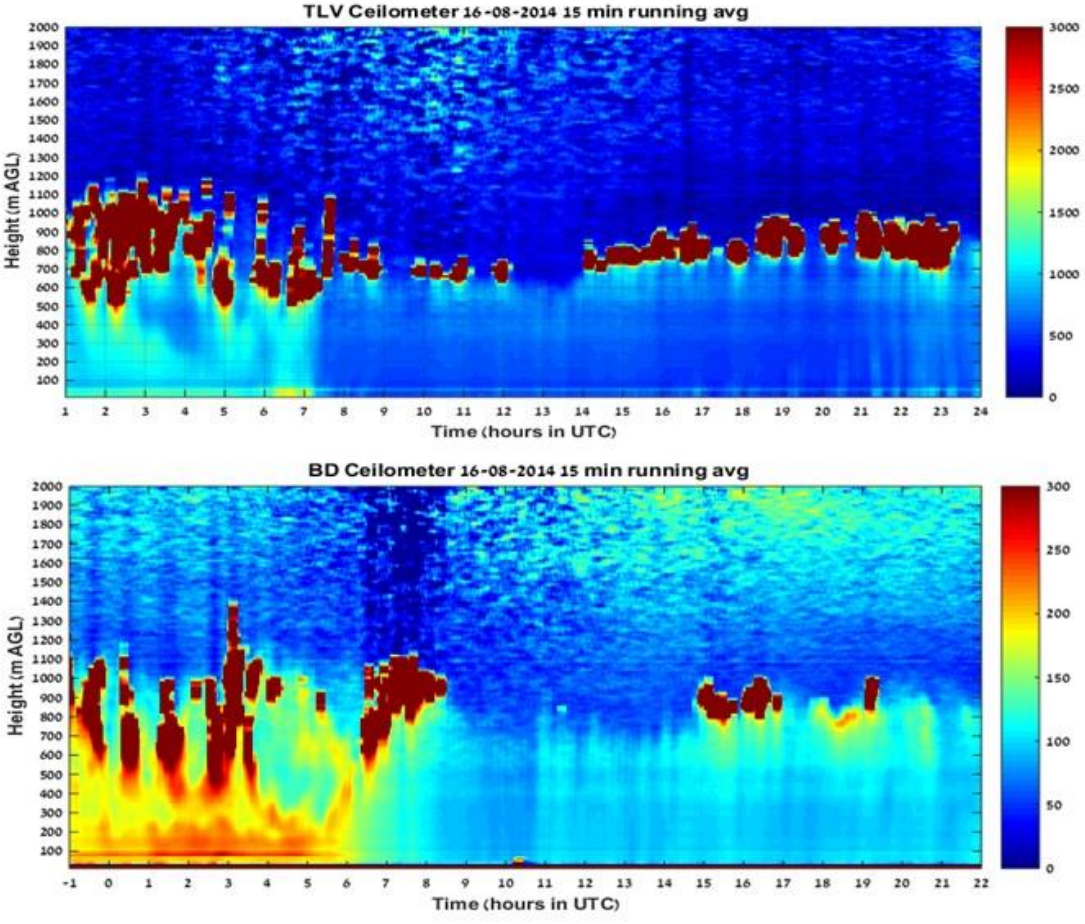

Figure 15. An example of difference in cloud cover on the 16.08.2014 measured by the onshore TLV ceilometer (top panel), and the inland BD ceilometer (bottom panel). The BD plot is shifted by 2hr to convert to UTC time.

Atmos. Meas. Tech. Discuss., doi:10.5194/amt-2016-85, 2016
Manuscript under review for journal Atmos. Meas. Tech.
Published: 12 May 2016

Atmospheric Measurement Techniques Discussions

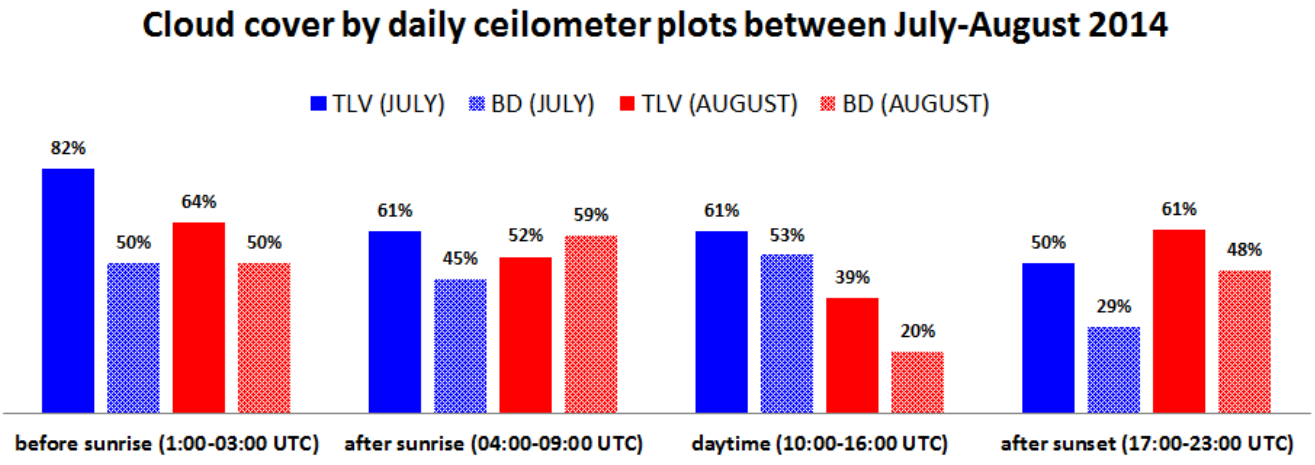

Figure 16. Cloud cover indications based on the daily 15 min running average plots from the TLV and BD ceilometers. Each plot was scored as follows: 1-consecutive cloud cover, .5- sporadic cloud cover, 0- no clouds. The evaluation was done on dates with full data from both ceilometers (19 days on July and 21 days on August).